

# Study on Damage Tolerance Behavior of Integrally Stiffened Panel and Conventional Stiffened Panel

M. Adeel

**Abstract**—The damage tolerance behavior of integrally and conventional stiffened panel is investigated based on the fracture mechanics and finite element analysis. The load bearing capability and crack growth characteristic of both types of the stiffened panels having same configuration subjected to distributed tensile load is examined in this paper. A fourteen-stringer stiffened panel is analyzed for a central skin crack propagating towards the adjacent stringers. Stress intensity factors and fatigue crack propagation rates of both types of the stiffened panels are then compared. The analysis results show that integral stiffening causes higher stress intensity factor than conventional stiffened panel as the crack tip passes through the stringer and the integrally stiffened panel has less load bearing capability than the riveted stiffened panel.

**Keywords**—Conventional Stiffened Structure, Damage Tolerance, Finite Element Analysis, Integrally Stiffened Structure, Stress Intensity Factor.

## I. INTRODUCTION

THE continual need for low acquisition cost and the emergence of high speed machining and other technologies has brought about a renewed interest in large scale integral metallic structures for aircraft applications. The high performance levels in machines and equipment continue to place more exacting demands on the design of structural components. In aircraft, where weight is always a critical problem, integrally stiffened structures have proved particularly effective as a lightweight, high strength construction. Integral fuel tanks and pressurized shells e.g. wing fuel tank, cabin pressurized fuselage usually create sealing problems for a riveted structure. These problems are eliminated to a large extent by integral stiffeners. Other advantages of integral stiffened structures over riveted panels are improved performance through smoother exterior surfaces by reduction in number of attachments, and nonbuckling characteristics of skin, increase in allowable stiffener compression loads by elimination of attached flanges and increased joint efficiencies under tension loads through the use of integral doublers, etc. Components in which the integrally stiffened structures can be employed are jet engine

components, aircraft and missile fuselages, jet engine pods, aircraft landing brake components, components with compound curvatures such as bulkheads and fairings, flat and curved panels, conical, and other shell-like components. Nevertheless, applications of low cost, large-scale integral structures in damage tolerance critical areas such as the fuselage have been inhibited by a perceived lack of damage tolerance and by cost and manufacturing risks associated with size and complexity of the parts.

In the Integral Airframe Structures (IAS) Program, a feasible integrally stiffened fuselage concept was developed and analyses and tests were run to validate equal or better performance than conventional designs with regard to weight and structural integrity, while achieving a significant reduction in manufacturing cost [1]. In NASA report Linear elastic analysis of integrally stiffened panel with circumferential crack was performed using NASTRAN and STAGS. Stiffeners and the pad-up region were all modeled in detail using shell elements. Linear elastic analysis results in straight line plots of load versus  $K_I$  at various crack lengths. It was found that as the crack approaches the thickness discontinuity at the stiffener base the stress intensity increases little with crack length. The analysis was also run with both NASTRAN and STAGS for a half crack length corresponding to a crack extending midway through the stiffener base on each side. Excellent agreement was found between two codes. While no further refinement of the model was done to more accurately evaluate the stress intensity in the vicinity of the thickness interface. The fracture analyses were conducted on the FAA/NASA stiffened panels using the STAGS code with the critical crack-tip-opening angle (CTOA) fracture criterion [2]. Comparisons were made between load-crack extension on stiffened and unstiffened panels with single cracks and multiple site damage (MSD). An assessment of the capability of the STAGS code with the critical CTOA failure criterion to predict residual strength was made. The results of residual strength pressure tests and nonlinear analyses of stringer-and frame-stiffened aluminum fuselage panels [3] with longitudinal cracks are presented. Two damage conditions are considered: a longitudinal crack located midway between stringers and a longitudinal crack adjacent to a stringer and along a row of fasteners in a lap joint that has multiple-site damage (MSD). At present it is readily possible to calculate the fatigue crack behavior, and particularly the residual

M. Adeel is with the Institute of Space Technology, Pakistan (phone: 0092-21-4933811; e-mail: adeelned2006@gmail.com).

strength of stiffened panels to a reasonable degree of accuracy provided the behavior of an unstiffened sheet of similar size is known [4]. The latter requirement does not set serious restrictions to the technical applicability of the method. Poe [5] predicted the crack growth behavior of a stiffened panel on the basis of unstiffened panel data, and compared his predictions with actual test data obtained from stiffened panels of different geometries. Poe's work contains many interesting results. It shows that a light stringer causes a smaller deceleration of crack growth, since it brings about less reduction of the stress intensity factor.

## II. DESCRIPTION OF STIFFENED PANEL GEOMETRY

This paper focuses on metallic integrally and conventional stiffened aircraft fuselage panels. Both types of the stiffened panels are constructed entirely of aluminum alloy. The structural configuration considered is shown in Fig. 1. The overall dimensions of the panel include a 1.98 m length and a 2.642m width. The skin is stiffened by 14-longitudinal Z-section stringers and two horizontal tear straps with a thickness of 4.32 mm. In the integrally stiffened panel, stringers are integrally machined with skin while a single line of rivets is used to attach stringer to the skin in conventional stiffened panel. The rivet spacing of one inch is used in the conventional stiffened panel.

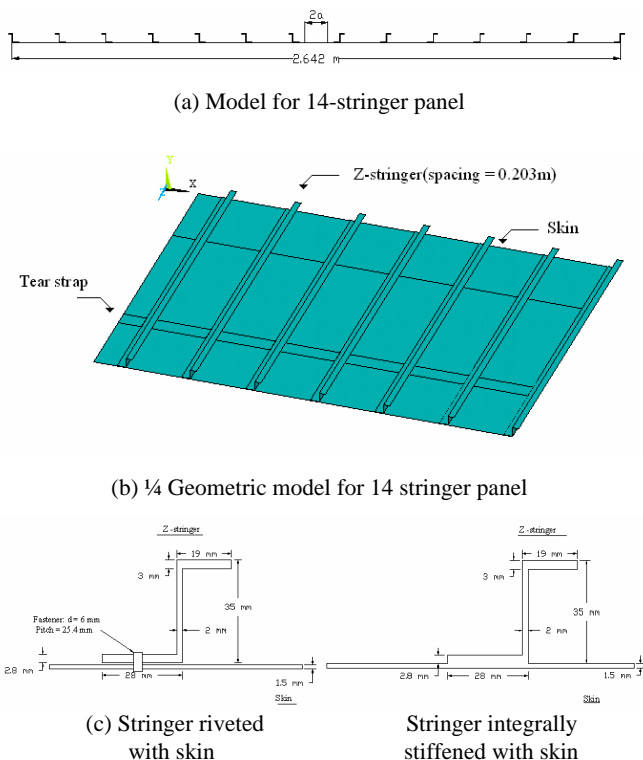


Fig. 1 Geometry of integrally stiffened panel and riveted stiffened panel

The physical properties of the model and loading are as under.

TABLE I  
 MATERIAL PROPERTIES

Symbol	Quantity	Values
$E$	Young Modulus	70 GPa
$\nu$	Poisson Ratio	0.3
$C$	Material Constant	$5 \times 10^{-11}$
$m$	Material Constant	3

TABLE II  
 LOAD MAGNITUDE

Symbol	Quantity	Values
$P$	Uniform Tensile Load	222.411KN

## III. FINITE ELEMENT MODEL DESCRIPTION

A quarter of both types of the stiffened panels with symmetric boundary conditions is analyzed using finite element analyses code ANSYS shown in Fig. 2 and Fig. 3. The SHELL181 element is used to model the skin and stringer in detail in both types of the stiffened panels. It is a 4-node element with six degrees of freedom at each node, translations in the x, y, and z directions and rotations about the x, y, and z-axes. It is finite strain element and is suitable for analyzing thin to moderately-thick shell structures. SHELL181 is well-suited for linear, large rotation, and/or large strain nonlinear applications. The rivets in the conventional stiffened panel are modeled using ANSYS spot weld feature based on the internal multipoint constraint (MPC) approach. This feature allows to model thin sheet components that are connected with spot welds, rivets, or fasteners. Singular elements are used around crack tip to pick up the singularity in the strain and stress at the crack tip. A circumferential crack is considered in the center of skin of both types of the stiffened panels and the same distributed tensile load is applied. The linear elastic static analysis is performed and stress intensity factor is calculated for both types of the stiffened panels. Similarly, stress intensity factor is obtained for various crack lengths while keeping same loading conditions. Stress intensity factor is also calculated for the unstiffened panel shown in Fig. 4 for different crack length which has the same cross section area as the stiffened panel. A graph of stress intensity factor ( $K_I$ ) vs. half crack length (a) is plotted for both types of the stiffened panels and the unstiffened panel shown in Fig. 6. The rate of fatigue crack propagation ( $da/dn$ ) is calculated using Paris law. Similarly, half crack length is plotted as function of rate of fatigue crack propagation shown in Fig. 7. In the conventional stiffened panel the more accurate von Mises stress around rivet and in the stringer hole is calculated using shell-to-solid sub modeling technique. The overall dimensions of the 3-D solid submodel include a 0.4064 m length and a 0.0508m width as shown in Fig. 8. The Solid 45 element is used to model the skin, stringer, and rivet in the 3-D solid submodel of the riveted stiffened panel. It is a eight node element with three degrees of freedom at each node: translations in the nodal x, y, and z directions. It is used for the 3-D modeling of solid structures. The element has plasticity, creep, swelling, stress stiffening, large deflection, and large strain capabilities. In 3-D solid sub model of the

riveted stiffened panel Surface-to-Surface contact elements i.e. CONTA174 and TARGE170 are used to model the contact between rivet, stringer, and skin. The 3-D solid sub model has same boundary condition as the 1/4 shell FE model of riveted stiffened panel while crack is not modeled. The nodal displacements are mapped from 1/4 shell FE model of riveted panel to this 3-D solid submodel. The nonlinear analysis is performed and von Mises stress is calculated around the rivet and in the stringer hole. Similarly von Mises stress is calculated for certain crack length. The half crack length is plotted as a function of maximum von Mises stress in the stringer hole as shown in Fig. 10. The fracture of both types of the stiffened panels and unstiffened panel takes place as stress intensity factor  $K_I$  reaches critical stress intensity factor ( $K_{Ic}$ ) corresponding to critical crack length ( $a_c$ ). The load bearing capability of both types of stiffened panel and unstiffened panel is analyzed by comparing the critical stress intensity factor of each stiffened panel and unstiffened panel with fracture toughness of the Aluminum alloy. Moreover the failure in riveted stiffened panel can also take place as the stress in the stringers hole reaches up to tensile strength of the material. Therefore failure of conventional stiffened panel is also analyzed by comparing the localize stresses in stringer hole obtained from 3-D solid submodel to that of the ultimate strength of the material.

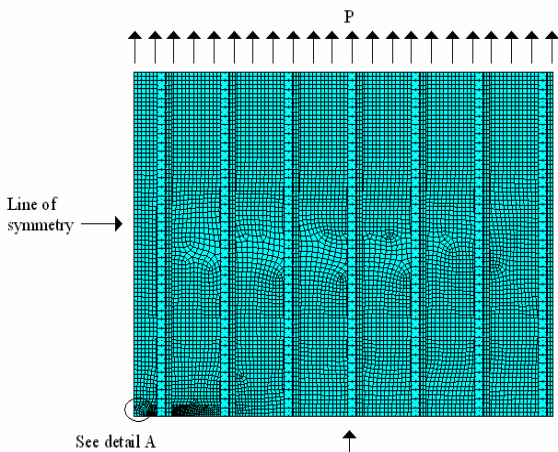


Fig. 2 1/4 FE model of riveted stiffened panel

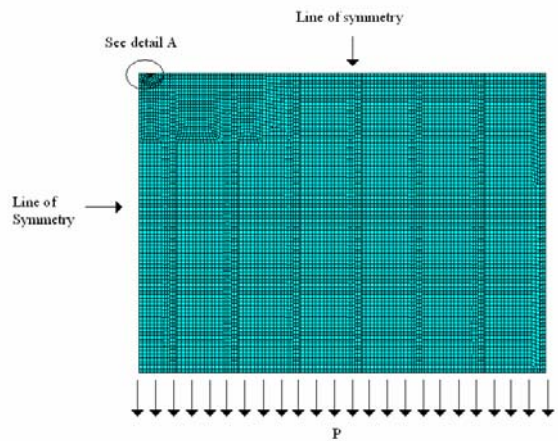


Fig. 3 1/4 FE model of integrally stiffened panel

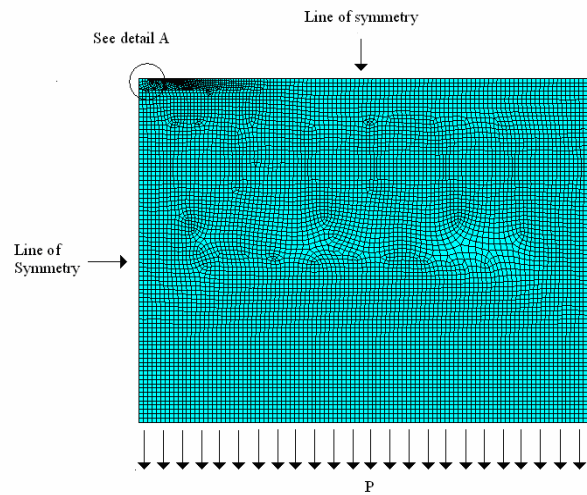
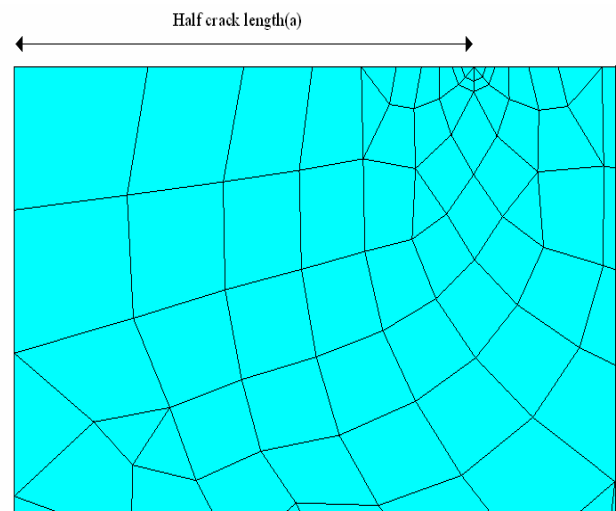


Fig. 4 1/4 FE model of unstiffened panel



Mesh near crack tip  
 Fig. 5 Detail A

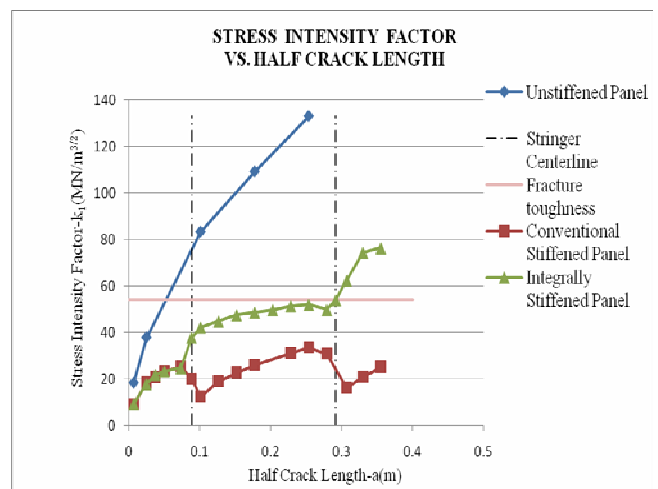


Fig. 6 Graph of stress intensity factor versus half crack length for riveted, integrally and unstiffened panels

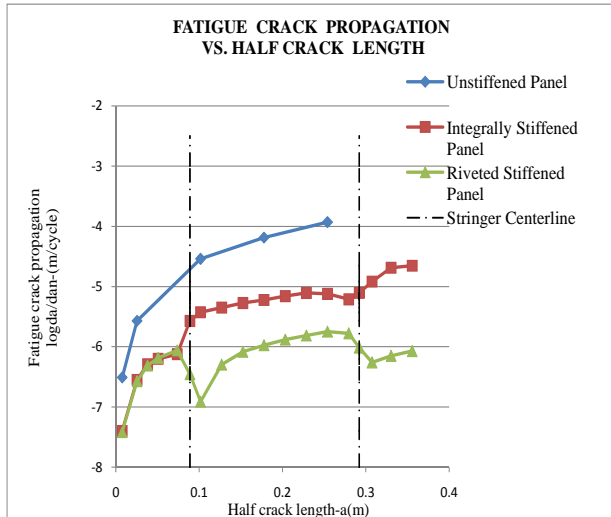


Fig. 7 Graph of fatigue crack propagation versus half crack length for riveted, integrally and unstiffened panels

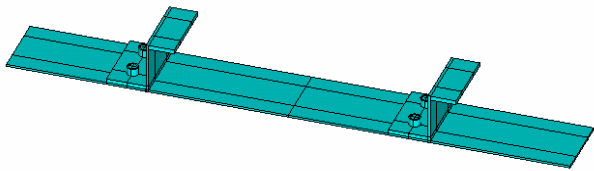


Fig. 8 Geometric 3-D solid Submodel for Conventional Stiffened Panel

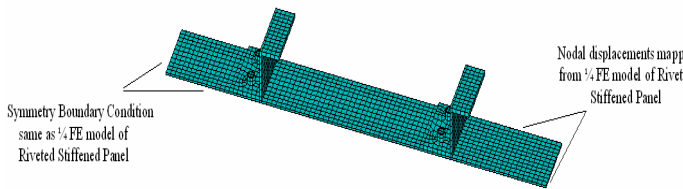


Fig. 9 FE 3-D solid Sub model for Riveted Stiffened Panel

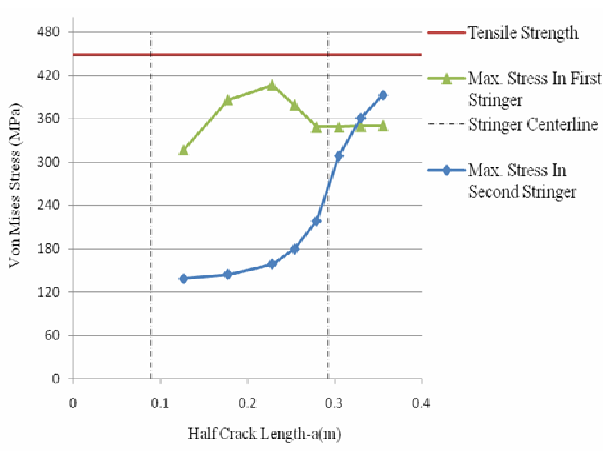


Fig. 10 Graph of Von Mises Stress versus half crack length for 3-D Solid Submodel of riveted Stiffened panels

#### IV. FINITE ELEMENT RESULTS

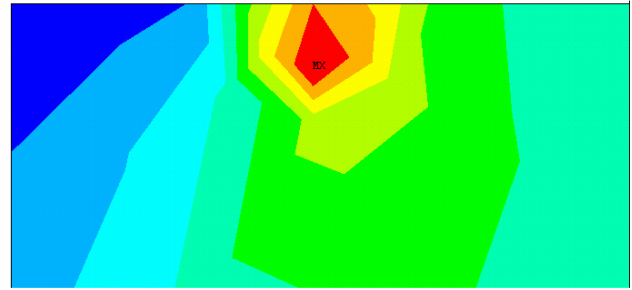


Fig. 11 Von Mises stress around crack tip

#### V. RESULTS DISCUSSION AND CONCLUDING REMARKS

The results depicted in Fig. 6 indicate that as long as the crack tip is far from stringer the stress intensity factor increases with same rate in both types of the stiffened panels with increasing crack length. However, in the integrally stiffened panel the stress intensity factor increases while in the conventional stiffened panel stress intensity factor decreases as the crack passes through stringer. Similar trend is observed as the crack tip approaches the second stringer in both types of the stiffened panels. When crack has passed the stringer, the stiffening effect decreases,  $K_I$  increases and so does  $da/dn$ . This trend is reflected by the plots in Figs. 6 and 7. In the case of integral stiffeners the stiffening element cracks simultaneously with the skin. The results in Fig. 7 show that integral stiffening causes less deceleration of crack growth compared to conventional stiffened panel as the crack passes through stringer. It is also found that the value of stress intensity factor in unstiffened panel is higher than that in the integrally stiffened panel for the same crack length. The existence of skin crack causes a load concentration in the stringer thereby enhancing the likelihood of stringer failure in the riveted stiffened panel. The finite element results of conventional stiffened panel show a rise in von Mises stresses in the stringer as the crack tip passes through it. The results in Fig. 10 depict that von Mises stresses in the first and second stringer hole are below the tensile strength of the material as the crack passes through the stringers in the 3-D solid sub model of the riveted stiffened panel.

The results presented in this paper indicate that integral stiffening causes higher stress intensity factor than conventional stiffened panel as the crack tip passes through the stringer. Consequently it can be concluded that in the case of integrally stiffened panel higher stresses will be developed around crack tip. It is also found that failure in the integrally stiffened panel takes place as the half crack length reaches up to critical crack length of 0.2921m corresponding to critical stress intensity factor of  $54 \text{ MN/m}^{3/2}$ . However, in the riveted stiffened Panel stress intensity factors are below the fracture toughness of the material and the von Mises stress in the stringer is also below the tensile strength of the material. It can be predicted from the above graphs that the integrally stiffened panel has less load bearing capability than the riveted stiffened panel. The finite element analysis method

used in this paper is verified by the results given in reference [1].

#### REFERENCES

- [1] R.G. Pettit, J. J. Wang, and C. Toh. Validated Feasibility Study of Integrally Stiffened Metallic Fuselage Panels for Reducing Manufacturing Costs, NASA/CR-2000-209342.
- [2] B. R. Seshadri, J. C. Newman, Jr., D. S Dawicke and R. D. Young. Fracture analysis of the FAA/NASA wide stiffened panels, NASA/TM-1998-208976.
- [3] Richard D. Young, Marshall Rouse, Damodar R. Ambur, and James H. Starnes, Jr. Residual strength pressure tests and nonlinear analyses of stringer- and frame-stiffened aluminum fuselage panels with longitudinal cracks, NASA no. 19990021207, 1998.
- [4] David Broek. Elementary Engineering Fracture Mechanics, Martinus Nijhoff Publishers, 1982,pp.408-433.
- [5] C. C. Poe. Crack Propagation in Stiffened Panels, ASTM STP 486, 1971.